Chapter 7
Exploring the Flooding Under Damming Condition in Punarbhaba River of India and Bangladesh

Swapan Talukdar, Swades Pal, Mohd Waseem Naikoo, and Atiqur Rahman

Abstract The flooding in India and Bangladesh causes enormous damage to life, property, and infrastructure loss. The present study, Punarbhaba River, a flood-prone transboundary river of India and Bangladesh, has witnessed many floods since historical times. It needs to be monitored closely. Therefore, we explored the flooding conditions and their effect on river ecology with management in the present study. The present study analyzed the flood condition using flood frequency, basic regional hydrology analysis, and probability analysis. We also reconstructed flooding scenarios using a 2-D hydraulic model at different flood return periods. The wetland transformation has been explored under the reconstructed flooding scenarios. The wetland habitat health was also modeled under different flood scenarios using logistic regression. We proposed flood management plans with the help of a random forest-based flood susceptibility model. Also, we proposed a wetland management plan in floodplain areas with a nature-based solution technique. The average water level (W.L.) during pre- and post-monsoon was 52% and 32%, respectively, but the flow level increased to 3% in postdam periods. The study area witnessed 18% more sudden flooding. Results showed that 4% and 5.1% wetland areas were predicted to be very high and high vulnerable zones during pre-dam conditions, while these have been increased to 34% (very high) and 20% (high) during postdam phase. Findings showed that the flood susceptibility model predicted 11.65% of the area as very high flood susceptible zones, which must be monitored closely. This study will provide a comprehensive foundation for flood management.

Keywords Hydrological alteration · Damming condition · Wetland habitat health · Nature based solution · Remote sensing · Machine learning

S. Talukdar · M. W. Naikoo · A. Rahman (✉)
Department of Geography, Faculty of Natural science, Jamia Millia Islamia, New Delhi, India
e-mail: arahman2@jmi.ac.in

S. Pal
Department of Geography, University of Gour Banga, Englishbazar, India

1   Introduction

Natural disasters and their consequences have increased in recent years due to poor environmental quality, climate change, rapid population growth, and artificial land use intensification (Tehrany et al., 2014). Natural disasters such as landslides, floods, earthquakes, and tsunamis cause significant damage, fatalities, property and infrastructure damage, economic losses, and social disturbance (Lee & Kim, 2018). Floods are one of the most devastating natural disasters in the world, causing damage to property, infrastructure, and human lives (Paul et al., 2019; Yalcin & Akyurek, 2004). Globally, floods have increased by 40% over the past two decades (Hirabayashi et al., 2013). Between 1995 and 2015, floods affected 109 million people and caused damage of up to $75 million in damage (Khosravi et al., 2019).

Floods occur when huge amounts of water exceed their carrying capacity and inundate river banks (Sarkar & Mondal, 2020). Climate change is often blamed for the increase in severe flooding (Gersonius et al., 2013). Floods are caused by both natural and human factors (Samanta et al., 2018). Climate change leads to changes in flood patterns, severity, and amplitude (Hens et al., 2018). Floods are common in the monsoon climate zone because of a highly irregular rainfall pattern (Wu et al., 2020). Floods are induced by rapid changes in channel shape due to agricultural expansion, drainage, settlement development, and piracy of distributaries, deforestation, and filling of wetlands (Dash & Punia, 2019). Artificial control, such as dam construction, reduces the magnitude of the flood, while the breach of levees increases the effect of the flood (Talukdar & Pal, 2017). Asian countries, such as India, have very weak flood prevention systems because of the high population density along the river bank and lack of infrastructural development (Du et al., 2019). Excessive rainfall, tidal surges, cyclone storms, strong current from dams and barrages, and inappropriate human intervention contributed to the floods in India (Samanta et al., 2018).

Leopold (1956) correctly predicted that the dam would be the primary contributor to a paradigm shift in the flow regime of rivers. For example, there were 427 large dams exceeding 15 m in 1900, 5268 in 1950, and 39,000 in 1986 (ICOLD, 1998). Currently, India has 5193 large dams, or 15% of the world's total (Graf, 1999). In the twentieth century, approximately 47,000 large dams (>15 m) and 800,000 small dams (World Commission on Dam, 2000) affected nearly half of the 292 significant river systems (Nilsson et al., 2005). Dams are increasingly common along rivers, in both developed and developing countries. Hence, the increasing artificial control over river flow dams has transformed natural flow into artificial (Garf, 2006).

The existence of floodplain ecosystem is inextricably linked to the overflow of periodic rivers of optimal size (Pal & Talukdar, 2019). Previous literature reported that the loss of repeated flood and new sediment deposition on a floodplain due to damming over the river causes changes in river processes and floodplain hydroecology (Paul & Pal, 2020; Talukdar et al., 2020). Regulated streamflow can limit the lateral expansion of river water (Pal & Talukdar, 2018), causing pressure in the habitat and ecosystem beyond the flood threshold.

The Punarbhaba River, a transboundary river between India and Bangladesh, is a highly important river in North Bengal, especially Dakshin Dinajpur, and some parts of Malda District (West Bengal, India) and the Dinajpur District of Bangladesh (Talukdar et al., 2023). Farmers in the basin area are dependent on it for irrigation, which is the only source of water. In addition, huge numbers of fishermen live in Dakshin Dinajpur District, who are totally dependent on it for livelihood. Most importantly, the Gangarampur town is situated along the bank of the river; therefore, this river meets the water requirement of the town. However, in 1992, a dam was constructed at Birganj (Bangladesh) over the river for fishing and irrigation. Since then, the river has witnessed a hydrological paradigm shift, which produces regulated and erratic flow. As a result, sporadic flooding occurred downstream. Therefore, effective flood management is crucial to prevent irregularities and frequent flooding downstream. Based on the obtained information, we determined to analyze and reconstruct the flooding scenarios of the Punarbhaba River. Therefore, to propose effective flood and wetland management in the study area, this research provided a comprehensive study of basic flood frequency analysis, statistical technique-based wetland habitat vulnerability under damming condition, and machine learning-based flood susceptibility to nature-based solution. To the best of authors' knowledge, this is the first attempt to provide a comprehensive study on wetland research under flood scenarios considering the damming condition.

2 Study Area

The Punarbhaba River Basin covers 5265.93 km^2 in India and Bangladesh. Punarbhaba is a 160 km river with a 3–8 km width (Fig. 7.1). It begins in Bangladesh's lowlands and goes through Dakshin Dinajpur's Gangarampur block (India). In India, it passes through four blocks of West Bengal (Gangarampur, Banshihari, Kushmandi, and Nalagola), while in Bangladesh, it passes through five districts (Panchagarh, Thakurgaon, Dinajpur, Bochaganj, and Biral). When the
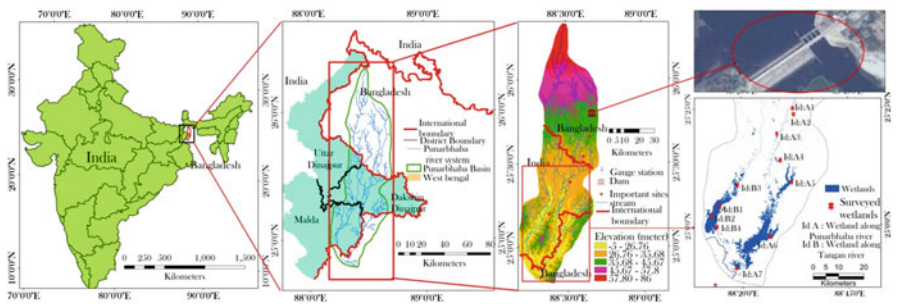

Fig. 7.1 Location of the study area with altitude and dam location. (Kamardanga dam, Birganj, Bangladesh)

Teesta River ran through it, it was hydrologically active. Neo-tectonic action diverted the Teesta flow toward Bangladesh, cutting off the Punarbhaba River (Rashid et al., 2015). This geological event caused a significant alteration in the river's and riparian environment's hydrological structure. Both ice and rain-fed perennial river flow became rain-fed seasonal river flow. Another source of flow changes in this river was the damming of the river in 1992 (Fig. 7.1). The riparian ecosystem has been severely affected in the post-hydrological modification period because of dam building in this river and considerable water lifting in such a densely populated region. This significantly influences the periodically inundated riparian wetlands, particularly those near the principal river. The dam installation causes dramatic changes. The river's cross-border difficulties between Bangladesh and India are additional causes to investigate its basin.

3   Historical Perspective of Floods in the Punarbhaba River

The Punarbhaba River is a small river compared with other rivers in West Bengal and India; therefore, the information is limited. However, the present research has prepared a historical flooding inventory based on the previous literature, local history, and government records. We found historical information about flooding about this river from the work of Agarwal and Narain (1991). They said that prior to 1787 the Teesta River flowed south (from Jalpaiguri to Dinajpur) through the Karatoya to the east, the Atreyee to the center, and the Punarbhaba to the west, where it joined the Ganga. Trisrota (three streams) was the name given to the three channels combined, which is today known as Teesta. In 1787, a disastrous flood occurred in Trisrota, which caused the Teesta River to change course and flow to the southeast, eventually flowing into the Brahmaputra River and separating from the Trisrota.

Subsequently, no data on flooding were available. However, the West Bengal Government's Disaster Management Department (https://ddinajpur.nic.in/) has retained flood data for the past 32 years. According to the archives, three types of floods have been recorded since 1987.

Floods of lesser intensity occurred in the following years: 1997, 1999, 2000, 2004, and 2005 (confined to water logging only).

Floods of moderate intensity occurred in 1987, 1992, 1995, and 1998.

In 2017, a severe flood occurred, killing 29 people and destroying Kutcha houses (fully, 40,996; severely, 12,477; and partially, 41,079; Hut-1309, animals, agricultural output, and other things).

4 Materials and Methods

4.1 Materials

In this present chapter, we used a variety of data collected from different sources. The river and road network was created from a Google Earth image. In ArcGIS, a drainage density map was created using the river network. Details of the materials can be found in Table 7.1.

4.2 Method for Flood Frequency and Magnitude Analysis

After dam construction (1992), the flood frequency and duration of high flow were determined. Fluctuations in water flow are studied closely to determine how they affect channel processes. It is possible to fit the lines through the data series with the Gumbel extreme value distribution (type 1). However, in artificially controlled

Table 7.1 Data types used for different purposes and their respective sources

Data type	Specification	Purpose	Sources of data
Water level data (1982–2016)	Three to six hour intervals in each day	Identifying missing flow, flood simulation	North Bengal Planning Division, Malda, Govt. of West Bengal
Landsat images (4–5 TM and 8 OLI)	Path/row: 139, 42, and 43; spatial resolution: 30 m. Pre-monsoon: 1980, 1982, 1983, 1985, 1986, 1987, 1988, 1989, 1990, 1991, 1993, 1995, 1996, 1997, 1998, 1999, 2000, 2001, 2004, 2005, 2006, 2008, 2009, 2010, 2014, 2015, 2017 Post monsoon: 1980, 1983, 1984, 1985, 1986, 1987, 1988, 1989, 1990, 1991, 1993, 1994, 1996, 1999, 2000, 2003, 2004, 2006, 2008, 2009, 2010, 2012, 2014, 2015, 2016, 2017	For wetland image preparation	USGS Earth explorer
SRTM DEM	Spatial resolution: 30 m	For generating surface	USGS Earth explorer
Wetland-related information	Depth of wetland, areas of wetlands, different land uses over the wetlands and its adjacent areas, channel linkage with wetlands, flood conditions on wetlands	For validating the result	Primary survey in Daiduba, Jatradanga, Jalakar Bithan and Bhatra wetlands along Tangon River; Gojamari and Bakla wetlands along Punarbhaba River

Collected from Talukdar and Pal (2021)

rivers, total probability techniques or other similar approaches should be used to explain flood probabilities better, as noted by Durrans (1988) and USACE (1993). In lieu of Gumbel's technique, a line graph of primary extreme flow distribution for each year was created, with primary, danger, and extreme danger levels (PDL, DL, and EDL) drawn on it. Flood frequency and magnitude have been approximated using this graphical method. On the normal graph, rating curves were created for both pre- and post-reservoir eras to identify changes in normal and critical flood-spilling discharge limitations and the pattern of inflection.

4.3   Instability of Flow

The instability index is used to comprehend continuous events or time-series data, such as river flow change. Significant changes in flow regime can be identified using instability analysis when water is diverted via a reservoir or canals. The instability index can well capture the internal variability and trend of flow data. Therefore, this method can detect dynamism in discharge data series. For detailed method, please see the work of Talukdar and Pal (2017).

4.4   Methods for Regional Hydrologic Analysis

Regional analysis of baseline hydrological conditions helps identify regional variance in the data series due to damming over the river. It is computed by comparing maximum/minimum annual flow ratios and maximum/mean flow ratios. The maximum/minimum flow ratio shows the flow range. This shows a significant degree of flow variability. It captures the basic hydrological essence of flows by comparing maximum and average daily flows over time. High max/mean ratios indicate rivers with high floods compared with typical flows, which result in complex geomorphology. Rivers with low max/mean ratios have less fluctuation in flow, simpler designs, and less change. Benn and Erskine (1994) recommended that water discharge be defined by a standardized percentage change (Pc).

In addition to this, Garf (2006) identified a few distinctive hydrological metrics for computing the regional hydrological situation under damming condition, such as maximum/mean daily flow, instantaneous minimum flow, one-day minimum flow, date of minimum flow, range of daily flows, mean up-ramp rate, mean down-ramp rate, etc.

4.5 Method for Simulating Flooding

A flood model can be created in one-dimension (1-D), two-dimensions (2-D), or three-dimensions (3-D). In the case of prismatic channels, the one-dimensional model is often used (channel with uniform cross-section). A two-dimensional model might be used to represent flood inundation as it travels through a non-prismatic channel (one with changing cross-section and alignment) such as a river, river overflowing, or floodplain (Al Amin et al., 2017). In this present chapter, we used HEC-RAS software, provided by the US Army Corps of Engineers, to model flood simulation based on 2-D hydraulic model. Three-dimensional hydraulic models describe flow parameters in three directions: longitudinal (along x), transversal (along y), and vertical (along z). Because of the high computing requirements, 3-D modeling is seldom used in hydraulic investigations. The 2-D hydraulic model, on the other hand, is reasonably time-efficient and straightforward, and it can display spatial flooding. Therefore, it has been frequently used worldwide. As a result, Tonina and Jorde (2013) suggested that 2-D modeling could be enough for most hydraulics and ecological applications.

The new HEC-RAS-v5 solves the complete 2-D Saint Venant equations and the 2-D diffusive wave equations:

$$\frac{\partial s}{\partial t} + \frac{\partial x}{\partial p} + \frac{\partial y}{\partial q} = 0 \tag{7.1}$$

$$\frac{\partial x}{\partial t} + \frac{\partial}{\partial p}\left(\frac{x^2}{h}\right) + \frac{\partial}{\partial q}\left(\frac{xy}{h}\right) = -\frac{n^2 x g \sqrt{x^2 + y^2}}{h^2} - gh\frac{\partial s}{\partial p} + xf + \frac{\partial}{\omega \partial p}\left(h\tau_{pp}\right)$$
$$+ \frac{\partial}{\omega \partial q}\left(h\tau_{pq}\right) \tag{7.2}$$

$$\frac{\partial y}{\partial t} + \frac{\partial}{\partial q}\left(\frac{y^2}{h}\right) + \frac{\partial}{\partial p}\left(\frac{xy}{h}\right) = -\frac{n^2 y g \sqrt{x^2 + y^2}}{h^2} - gh\frac{\partial s}{\partial q} + yf + \frac{\partial}{\omega \partial q}\left(h\tau_{qq}\right)$$
$$+ \frac{\partial}{\omega \partial p}\left(h\tau_{pq}\right) \tag{7.3}$$

where h is the water depth (m), x and y are the specific flow in the p and q directions (m^{2}s1), s is the surface elevation (m), g is the acceleration due to gravity (m s2), n is the Manning resistance, is the water density (kg m^3), and f is the Coriolis (s1). The inertial components of the momentum equations (Eqs. 7.2 and 7.3) should be neglected while choosing the diffusive wave (Quirogaa et al., 2016).

For computing flood simulation modeling (FSM) or flood reconstruction model at different return periods, the cumulative discharge of maximum flow level at Haripur and Bamangola Gauge stations has been used.

4.6 Method for Wetland Mapping

Extraction of objects from satellite based on spectral value is not new methods. There are several spectral indices that are available for extracting water-bodies, such as Normalized Difference Vegetation Index (NDVI) (Townshend & Justice, 1986), the Normalized Difference Water Index (NDWI) (McFeeters, 1996), the Modified Normalized Difference Water Index (MNDWI) (Xu, 2006), the Water Index (WI), and so on. All these techniques have some advantages and disadvantages. Therefore, before using the spectral indices, researchers have to conduct pilot study and confirmed about the indices. In the present study, Das and Pal (2016) have conducted a study for extracting water bodies from spectral indices. They reported that NDWI is the best method for detecting water bodies and established the optimal threshold for distinguishing water bodies from nonwater bodies in the present study area. As a result, in the present study, we used NDWI with a thresholding approach to map the time series wetland areas.

4.7 Method for Wetland Habitat Vulnerability Under Flooding Conditions Considering Damming Effect

Wetland habitat vulnerability is crucial for wetland management and conservation. The ecological vulnerability assessment approach is often used to analyze wetland degradation risk and vulnerability (Walker et al., 2001). Researchers have frequently used several framework to calculate the habitat vulnerability, such as USEPA's "Three-Step Framework" (USEPA, 1998), PETAR (Moraes & Molander, 2004), RRM (O'Brien & Wepener, 2012), and PSR (Islam et al., 2021).

The pressure, state, and response (PSR) model were devised by Rapport and Friend (1979), and it was extensively expanded by the Organization for Economic Cooperation and Development (1993). This model has effectively monitored the conditions of marsh, forest, river, and other natural resources. Since the model established a cause-and-effect link between physical and anthropogenic indicators, it can accurately model the wetland habitat vulnerability.

We selected seven parameters to assess wetland habitat vulnerability, such as water presence frequency, agricultural presence frequency, fragmentation of wetland bodies, built-up indices, wetland change rate, flood inundation model or flood reconstructed model, and nonpermanent pixel frequency. To build wetland vulnerability models, selected factors are collected for both before and after dam phases. Then, all the parameters have been integrated together using logistic regression model to generate the habitat vulnerability assessment. It is a multivariate analytic model that predicts several predictor variables to estimate the probability of a dichotomous or binary event (presence or absence). It is used to discover the model that best fits a dependent indicator (vulnerability) and a collection of independent indicators (continuous, discrete, or both) (Basu & Pal, 2017). However, it

does not need linearity or equal variances in the independent indicators' relationships (Solaimani et al., 2013). It is recommended to employ an equal number of vulnerability and non-vulnerable sample sites to establish a better sampling pattern (Suzen & Doyuran, 2004). Therefore, in the present chapter, we selected 1500 wetland vulnerable points and similar number of non-vulnerable points (details can be found in Talukdar & Pal, 2018). We split the dataset into 83:17 ratio as training and testing datasets for model building and validation.

Further, we validate the wetland habitat vulnerability model using ROC curve. It plots the true positive rate against the false positive rate of various diagnostic tests cut points. The area under the ROC curve measures the goodness of fit. The accuracy has been judged based on the area values under the curve (AUC). It ranges from 0 to 1. Close to 1 shows very high accuracy and vice versa (Rasyid et al., 2016).

4.8   Method for Flood Susceptibility Model

Flood susceptibility mapping is crucial in the present study for flood prevention and control. Therefore, we chose 12 flood conditioning factors for flood susceptibility modeling, such as elevation, slope, aspect, curvature, flow direction, flow accumulation, Stream Power Index (SPI), Normalized Difference Water Index (NDWI), Normalized Difference Vegetation Index (NDVI), Normalized Difference Moisture Index (NDMI), and Normalized Difference Built-up Index (NDBI).

Alike wetland habitat vulnerability modeling, flood inventory is also required to predict flood susceptibility. We collected the flood and non-flood locations from the field survey and historical Google Earth Image. All flood conditioning variables and flood inventories were integrated with machine learning algorithm (random forest) to generate a flood susceptibility map. Breiman (2001) invented random forest, a widely used robust ensemble machine learning approach used for regression, classification, and unsupervised learning. It is widely used in natural hazard modeling, hydrology, LULC categorization, and finance (Sevgen et al., 2019).

The random forest model combines the random subspace and bagging ensemble models (Naikoo et al., 2023; Chen et al., 2020). This model is less sensitive to multicollinearity and can manage imbalanced and missing data. The RF model works by:

1. Generating subsets from the original datasets using bootstrap-based re-sampling.
2. Producing decision trees using the subsets.
3. Combining the classification or prediction results from all decision trees.

The number of decision trees (Ntree) and the characteristics of the candidate included in the subsets (mtry) are claimed to affect the performance of the RF method (Chen et al., 2020). A considerable Ntree value may increase modeling durations, whereas a little amount might cause problems.

The generated flood model has been validated using ROC curve as like wetland vulnerability model.

4.9   Method for Wetland Creation and Restoration Using Nature-Based Solution

In this work, we used a nature-based solution method to restore and protect a wetland. To do so, we first selected wetland restoration and conservation areas based on a variety of surface water, topographical, water quality, and land cover factors. Then, we created wetlands in the GIS platform on the appropriate places in vector form. Then, we rasterized the new wetland map with base resolution from the polygon format. Finally, we used new wetland model with other parameters to evaluate the wetland habitat vulnerability condition using logistic regression model.

5   Results and Discussion

5.1   Monitoring Flooding Conditions in the Punarbhaba River

Storage of reservoirs delays and reduces downstream flooding (Williams & Wolman, 1984), although the delay varies with reservoir size and operational restrictions (Kondolf, 1994). The maximum flood peaks (66%) in pre-dam condition occurred during the pre-monsoon months; however, peak water levels are reduced in postdam condition. Over the past 37 years, the pre-monsoon months have witnessed 55% reduction in the peak discharge. Despite the fact that the dam's storage capacity is only 6,540,000 cubic meters, large volumes of water are channeled through canals for farming, lowering peak discharge levels. Figure 7.2 also shows the frequency of peak flows during the monsoon months. The modal discharge class is also shown on
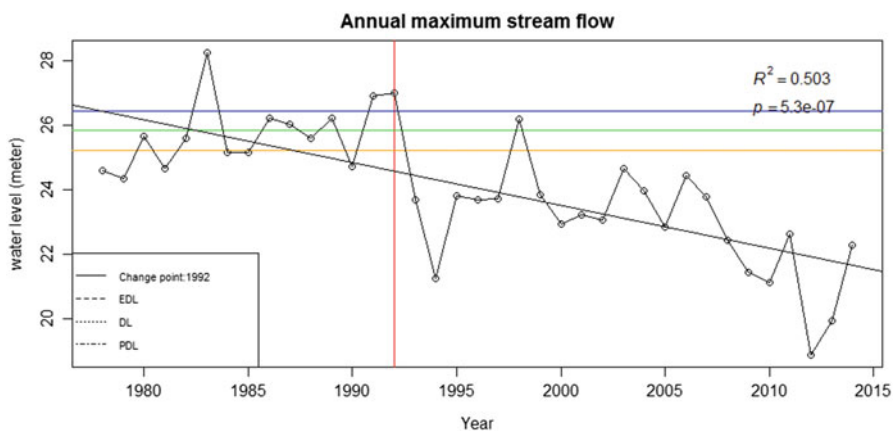

Fig. 7.2 Annual streamflow level in different years in reference to primary danger level (PDL), danger level (DL), and extreme danger level (EDL)
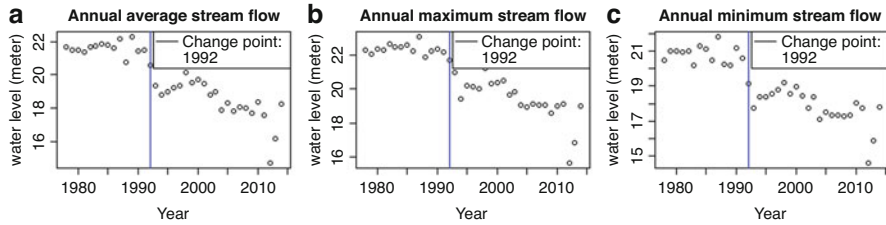
Fig. 7.3 Location of change point in annual (**a**) average water level, (**b**) maximum, and (**c**) minimum streamflow data (1978–2016)

this graph. It also displays the months with the highest concentration of discharge. We found that the maximum water level (24–26 m) frequency in pre-dam condition was 10 times, but in postdam condition, the height of maximum water flow has reduced to 22–24 m. The frequency was 13 times in 26 years of postdam period. It is surprising to know that the discharge has reached to 28 m just once in pre-dam condition. Since then, the river has never got that level. According to a flood frequency analysis, only three times (20% of the 15 years) had water levels over the extreme danger level (EDL = 26.42 m). However, after the dam construction, water levels are constantly lower than the EDL. Only one year (1998) exceeded the DL (Fig. 7.2). These evidences indicate that the number of flood peaks has decreased since the reservoir was built.

Furthermore, the average annual streamflow levels at pre- and postdam conditions were 21.55 and 18.43 m, respectively (Fig. 7.3). The average water level has declined by 3.12 m since the dam was built. Following the damming in 1992, trend analysis was carried out in order to compare the pattern from before to after the change point.

On average, during the monsoon, maximum high flow duration has decreased by up to 73%, while the diurnal fluctuation coefficient of discharge has increased by 37%. Maximum and mean flow ratios have dwindled in reservoirs condition. After damming, the Punarbhaba River has a large (63.89%) shift in flow (Table 7.2).

The Punarbhaba River's flood probability and return period with specific magnitudes were estimated using Gumbel's extreme value distribution method (Table 7.3). Figure 7.4a, b show the recurrence interval curves for the Punarbhaba River concerning flow magnitudes and the best-fit approach for selection. According to this result, the probable water level in the Punarbhaba River in 2 years return period would be 21 m. The water level of the river would be 30 m at 50-year return periods (Table 7.3).

5.2 Reconstruction of Flooding Under Damming Scenario

The flood levels for varied return durations were utilized to simulate spatial floods. Figure 7.4a–e shows flooded areas at 2, 5, 10, 25, and 50 years of return period. The

Table 7.2 Hydrological parameters for regional analysis in pre- and postdam conditions

Hydrologic parameters	Before reservoir(1978–1992)	After reservoir(1993–2014)
Instantaneous maximum flow (number)	08	16
Year of instantaneous maximum flow	1981, 82, 83, 84, 86, 89, 91	1995, 96, 97, 99, 2001, 03, 04, 06, 08 (January), 08 (June), 10 (January), 10 (June), 11,13, 14
Thirty-day maximum flow	28.47 m	23.8 m
Month of maximum flow	August 1983	September 1998
Mean monthly flow	21.55 m	18.35 m
Instantaneous minimum flow (number)	7	14
Year of instantaneous minimum flow	1981, 82, 83 (March), 83 (September), 86 (June), 86 (December), 89, 91 (May), 91 (November)	1993 (April), 93 (November), 98, 2001, 02 (March), 02 (December), 03 (February), 03 (September), 06 (March), 06 (August), 06 (December), 09, 2012
Thirty-day minimum flow	14.83 m	11.87 m
Month of minimum flow	May 1991	March 2013
Range of flows (max.-min.)	17.78–28.47 m (during1983)	18.07–23.8 m (during 1998)
Mean up-ramp rate of water level	1.45 m/month	1.40 m/month
Mean down-ramp rate of water level	1.35 m/month	1.25 m/month
Number of high flow pulses above PDL (P.D.L. = 25.22 m)	12	0
Year of high flow pulses	1983 (July), 83 (August), 86, 87 (July), 87 (August), 87 (September), 89 (July), 89 (September), 89 (October), 91, 92 (July), 92 (August)	–
Number of low flow pulses	9	17
Year of low flow pulses	1882,83,86,87,88,89,90,91,92	1995,96,99,2001,02,03,04,05,06,07,08,09,10,11,12,13,14

Collected from Talukdar and Pal (2017)

Table 7.3 Estimation of the return periods and flood magnitudes with Gumbel extreme value and log-Pearson type III

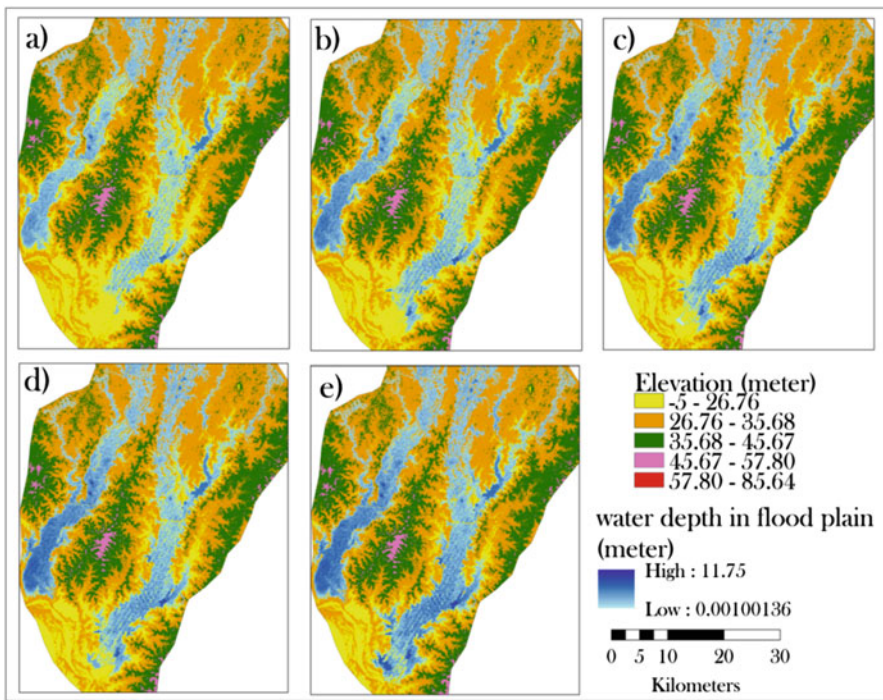| Return periods (years)	Percent of chance	Punarbhaba (water level in meters)	
		Gumbel	Log-Pearson type III
2	50	23.68	24.13
5	20	25.73	25.8
10	10	27.06	26.63
25	4	28.78	27.48
50	2	29.98	28.01
100	1	31.24	28.47
200		32.40	28.88

Collected from Pal and Talukdar (2019)

Fig. 7.4 Reconstruction of flooding scenarios using 2-D hydraulic model at (**a**) 2 years, (**b**) 5 years, (**c**) 10 years, (**d**) 20 years, and (**e**) 50 years return periods

areal extent and depth of floodwater in flooded areas for Punarbhaba Rivers were also calculated, such as 737.63 km^2 flooded areas with water level of 29.98 m (recurrence interval 50 years), 671.14 km^2 with water level of 28.78 m (recurrence interval 20 years), 634.83 km^2 with water level of 27.07 m (10 years interval), and 597.66 km^2 with water level of 25.73 m (5 years interval). We found that high discharge caused higher extent of lateral flooding. Based on this, we classified the

lateral flooded areas as active flooded areas (5 years of return period) because these regions would get flood water in every 5 years interval, dormant flooded areas (20 years), and moribund flooded areas (50 years). We also computed the lateral expansion of flooded areas in pre- and post-conditions. It is found that huge parts of active floodplain (found in pre-dam period) have transformed into dormant and moribund flooded areas.

Punarbhaba River has a maximum lateral flood reach of 10 km, and the right bank extends even farther. For 50 years, the lateral flood extent (width) of this basin at the confluence section is 7.7 km; for 10 years, the lateral flood extent (width) is 5 km; and for 5 years, it is 3.9 km. A flood breadth of 7.7 km in pre-dam conditions was reduced to 3.36 km after a dam was built.

5.3 Impact of Flooding Under Dam Condition on Wetland Habitat Vulnerability

Figure 7.5a depicts the current wetland cover across floodplain at pre- and postdam conditions. Figure 7.5b, c show the wetland status before and after the dam. As noted in the methodology section, they are categorized as safe, stress, and critical wetland based on the frequency of receiving floodwater from the river. The wetland area decreases in postdam condition from 215.70 km^2 to 90.40 km^2. The majority of the lost water body is turned into farmland. From pre-dam to postdam, the percentage of safe, stress, and critical wetland decreased from 69.09% to 53.80%, 19.95% to 25.50%, and 10.96% to 20.71%. It means that 53.80% of wetland now gets regular water from the concerned rivers. The percentage of the wetland now in a stress zone is 5.55%. These regions are beyond the current flood limit but not above the pre-dam flood limit. Approximately 9% of wetland area is in critical condition due to
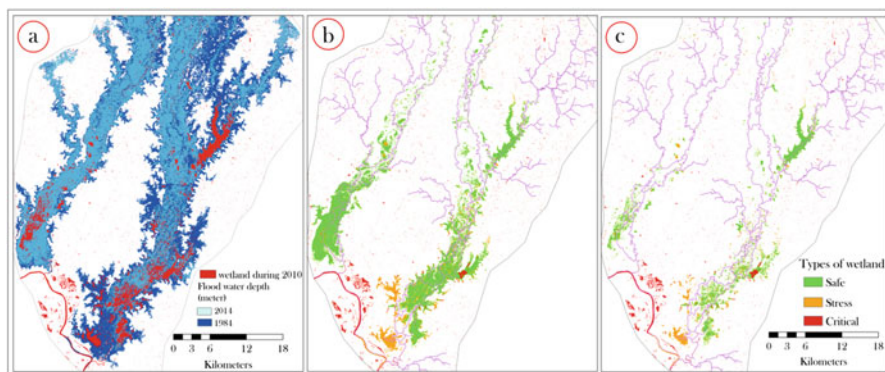

Fig. 7.5 Effect of flooding under damming scenario on the floodplain wetlands: (**a**) active floodplain for pre- and postdam condition, (**b**) wetland states during pre-dam, and (**c**) postdam periods

exceeding flooding threshold of pre-dam periods. Wetlands without inundation water in a controlled environment are changing. Most species will likely relocate to other wetlands with reliable water supplies. The research area's wetland is becoming more hydro-ecologically vulnerable. Reduced flooded areas and increased flood irregularity are the main reasons for increasing habitat vulnerability. Rainfall has not decreased much in this region during the previous 50 years. Thus, the dam's flow control is critical for such rapid wetland degradation.

We also assessed the health condition of the wetlands under flooding and other factors for pre- and postdam conditions. Before integrating all seven data layers, each indicator's geographical variation status may be quantified to better understand the control of each indicator on the final integrated vulnerability layer. The LWPF area increased by 3.32% following dam construction, showing that these areas experienced water scarcity and isolation from the channel. This indicates that, after dam building, about half of the wetland area had low depth water availability and quickly dried up, exposing it to damage, i.e., vulnerable wetland existence. Patch and edge areas rose from 11.61 to 13.65% and 23.37 to 24.46%, respectively, after dam building. Increased patch and edge wetland area imply decreasing core wetland area due to increasing disturbance, resulting in wetland susceptibility. The area of >80% wetland conversion increased by 23–25% from pre- to postdam; the area of high agriculture presence frequency increased by 23–25% from pre- to postdam, indicating that permanent agricultural land was extended by converting low water presence and low water depth flood plain region. In the NDBI dataset, there was evidence of built-up areas encroaching into the marsh. Because the susceptible zone in each dataset is not concentrated in the same geographical unit or because these datasets exhibit spatial variability, it is necessary to aggregate these datasets using the weights established by the FR and LR models.

Before aggregating the selected seven indicators, the geographical discrepancy condition of each indicator may be stated to assess the impact of each sign on the vulnerability state.

This study uses logistic regression to analyze the spatial relationship between the wetland's irregular and low water presence frequency zones and the conditioning factors (WPF, FIM, NPW, APF, FoW, NDBI, and WC). Figure 7.6 shows the composite LR models of physical wetland vulnerability before and after dams. When the components are combined, WVI maps for pre- and post-dam eras are constructed. A value of extremely low, low, moderate, high, or very high is computed (Fig. 7.6). A higher WVI indicates more susceptibility. The model predicts that pre-dam wetland areas of 7.44 km^2 (3.82%) and 9.78 km^2 (5.02%) are very high and highly vulnerable, whereas postdam regions of 42.97 km^2 (34.07%) and 25.46 km^2 (20.19%) are very high and extremely vulnerable. LR models also reveal that a large quantity of wetland is now vulnerable. Migratory birds prey on marginal and little wetlands.
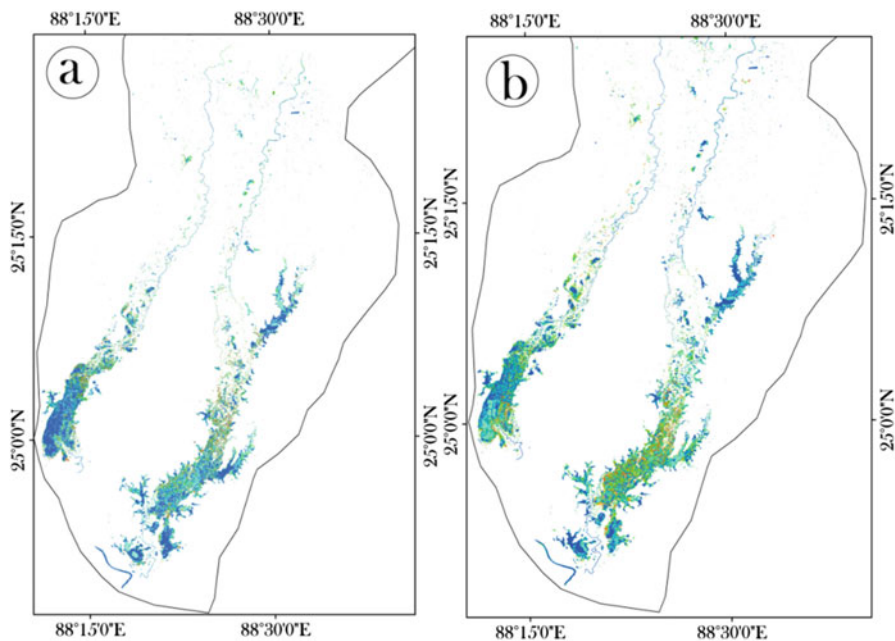
Fig. 7.6 Wetland habitat modeming under flooding condition using LR model for (**a**) pre- and (**b**) postdam condition

5.4 Drivers for Flooding

Floods are often classified as natural disasters whether catastrophes are classified as natural or man-made. Floods, for example, are listed under the subhead "natural catastrophes" by the National Institute of Disaster Management. Floods are sometimes referred to as "the most common sort of natural catastrophe" by the World Health Organization. As like earthquakes, landslides, avalanches, storms, and tsunamis, floods have been a component of the earth's natural system since the dawn of time. Human activity, on the other hand, has been directly contributing to floods since the advent of agriculture and urbanization. We did, however, provide a list of causes for flooding.

Floods caused by a dam failure and breaching are abrupt, and their effects are more damaging to lives and property due to the intensity of the flood and the unpreparedness of the inhabitants of the surrounding regions. Communities are vulnerable due to the unexpected nature of flooding caused by dam failure and the reluctance of the authorities to share information with the public. Flood water rises in an undammed river not suddenly, but with time, giving people time to react. Furthermore, the dam alters the riverbed's contours, the river's down streamflow, and even the floodplains.

The gradual shrinking of wetlands and lower water level are making it easier for farmers to reclaim wetlands for agricultural purposes. According to Pal and Talukdar (2018), the agriculture area of the Punarbhaba River increased from 59.19% to 84.2% (out of total basin area) in postdam condition, while the built-up area is increased from 2.54% to 5.72%. Many researchers, such as Pal and Saha (2018), have reported on the conflict between farmland and wetland. As a result of decreasing wetland areas (act as natural water container), the study area has experienced flooding with less amount of rainfall (e.g., flooding at Gangarampur along the Punarbhaba river on 14 August, 2017). As per the government report, damages were more in 2017 flood with 26 m water level recorded at gauge station, while 1987 flood caused less damage with 28 m recorded water level. The major factor is the decrease of wetland water storage capacity.

5.5 Recommendation for Flood and Floodplain Wetland Management

5.5.1 Flood Susceptibility Model

The flood susceptibility model has been prepared for future flood management to reduce the damage. Landsat image and SRTM DEM datasets were used to create flood conditioning parameters, which were used to prepare susceptibility model using RF. Following natural break principles, the generated flood susceptibility model was divided into five susceptibility zones: very high, high, moderate, low, and very low (Fig. 7.7). The model identified riparian corridors along major rivers as very high flood-prone zones, accounting for 7–15% of the overall area. The high flood susceptible zone, on the other hand, changes only 15–16% (smaller
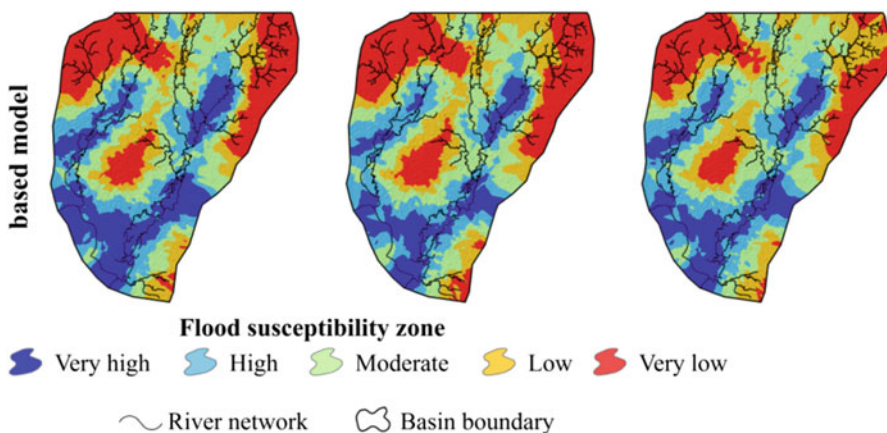

Fig. 7.7 Flood susceptibility model using RF at different tree number

fluctuation), yet the variance is large (area: 19–26%). The distant from major rivers and interfluves zones of the major rivers have very low and low flood sensitive zones. Low and extremely flow flood-sensitive zones have been discovered in around 16–25% and 32–44% of the areas, respectively.

5.5.2 Wetland Conservation and Restoration Using Nature-Based Solution

The first task was to predict the appropriate location of the wetland to be restored and conserved. For this, wetland restoration and conservation suitability model was constructed using several factors and analytical hierarchy process (AHP) model. The AHP model has calculated weights for different parameters based on expert opinion and pair-wise matrix comparisons. Then, the weights were assigned to the factors and generated wetland restoration and conservation suitability map. The map was classified into three classes, such as less suitable, somewhat appropriate, and very suitable. We selected the very suitable class for the best choice of the wetland conservation and restoration. The less suitable and somewhat appropriate groupings are dominated by agricultural land and other land use/land coverings (Fig. 7.8). Agricultural landscapes and towns inhibit the creation of new wetlands by fragmenting existing wetlands, putting habitat quality and wetland health at risk. As a consequence, human intrusion should be avoided in newly developed wetlands. The areas with the worst quality require extra conservation efforts. Then, we converted this class into polygon format and combined it with the existing wetland map. Thus, we created a new wetland map, which then rasterized in ArcGIS software.
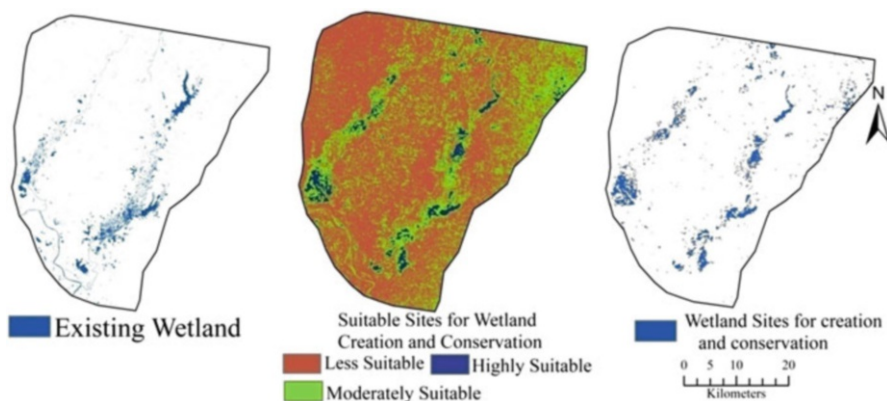

Fig. 7.8 Modeling of suitable sites for wetland conservation and restoration: (**a**) existing wetland (2020), (**b**) suitable site model, and (**c**) selected sites for wetland conservation and restoration (N.B. highly suitable site for wetland conservation and restoration has been selected as wetland conservation and restoration sites)
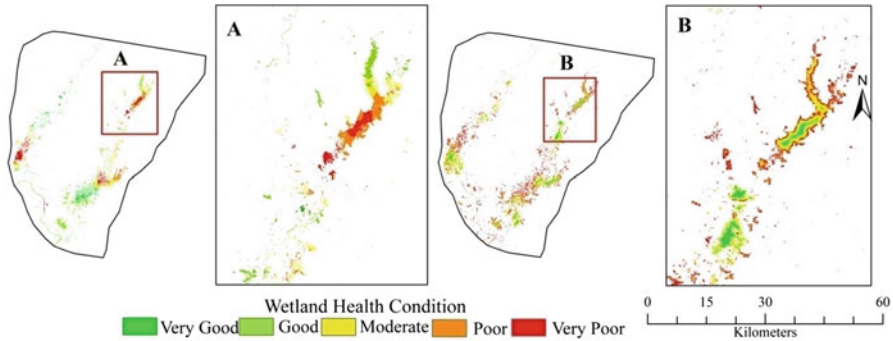
Fig. 7.9 Comparisons of wetland health condition models between (**a**) health condition model using existing data and (**b**) health condition model using existing data and new wetland data (N.B. new wetland map has been prepared by integrating existing wetland area (2020) and selected sites for wetland conservation and restoration)

Then we used new wetland map as parameters for wetland habitat health condition modeling with other parameters. Thus, we created two wetland habitat health condition models, such as the current condition and the new condition (Fig. 7.9). Figure 7.9 shows the health of wetland habitats using existing data (Fig. 7.9a) and the health of freshly developed wetland data using existing data (Fig. 7.9b). The facts that Fig. 7.9a depicts regions dominated by poor and very poor wetland health, while the percentage of poor and very poor areas decreased dramatically when new wetland data was included, is a remarkable finding. The area of superior quality wetland, on the other hand, has increased from 28% in current wetland data to 62.28% using new wetland data. The state of wetlands would undoubtedly improve if additional wetlands could be developed in a sustainable way.

6   Conclusion

It is obvious from this study that the Punarbhaba River has seen hydrological changes as a result of the dam's construction. As a result, the average water level has decreased from 42% to 62%. As a result, the river's floodplain wetlands, which are mostly nourished by river water, have faced water shortage. It results in a large reduction in the marsh area. Factors such as agricultural growth, continual urbanization, groundwater depletion, river separation, and other developmental projects hasten the process. Existing wetland vulnerability is considerable, according to the data. Sudden and erratic floods have been reported in the research region as a result of damming. As a result, flood vulnerable mapping has been completed in order to monitor the floods. The lower reaches of the river basin, particularly the very close riparian corridor of the main river, which accounts for 19% of the overall study area, has been determined to be very vulnerable to flooding. These locations must be closely monitored. We also recommended adopting the natural-based solution approach for flood and wetland managements.

References

Agarwal, A., & Narain, S. (1991). *Floods, flood plain and environmental myths* (State of India's environment: A citizens' report, 3) (pp. 32–39). Centre for Science and Environment. http://csestore.cse.org.in/usd/soe3.html

Al Amin, M. B., & Haki, H. (2017). Floodplain simulation for Musi River using integrated 1D/2D hydrodynamic model. In *MATEC web of conferences* (Vol. 101, p. 05023). EDP Sciences.

Basu, T., & Pal, S. (2017). Exploring landslide susceptible zones by analytic hierarchy process (AHP) for the Gish River Basin, West Bengal, India. *Spatial Information Research, 25*(5), 665–675.

Benn, P. C., & Erskine, W. D. (1994). Complex channel response to flow regulation: Cudgegong River below Windamere Dam, Australia. *Applied Geography, 14*(2), 153–168.

Breiman, L. (2001). Random forests. *Machine Learning, 45*(1), 5–32.

Chen, T., Zhu, L., Niu, R. Q., Trinder, C. J., Peng, L., & Lei, T. (2020). Mapping landslide susceptibility at the Three Gorges Reservoir, China, using gradient boosting decision tree, random forest and information value models. *Journal of Mountain Science, 17*(3), 670–685.

Das, R. T., & Pal, S. (2016). Spatial association of wetlands over physical variants in barind tract of West Bengal, India. *Journal of Wetlands Environmental Management, 4*(2).

Dash, P., & Punia, M. (2019). Governance and disaster: Analysis of land use policy with reference to Uttarakhand flood 2013, India. *International Journal of Disaster Risk Reduction, 36*, 101090.

Du, S., Cheng, X., Huang, Q., Chen, R., Ward, P. J., & Aerts, J. C. (2019). Brief communication: Rethinking the 1998 China floods to prepare for a nonstationary future. *Natural Hazards and Earth System Sciences, 19*(3), 715–719.

Durrans, S. R. (1988). 18. Total probability methods for problems in flood frequency estimation. In *International conference on statistical and Bayesian methods in hydrological sciences in honor of professor Jacques Bernier, Paris, Paris, France* (pp. 299–326).

Gersonius, B., Ashley, R., Pathirana, A., & Zevenbergen, C. (2013). Climate change uncertainty: Building flexibility into water and flood risk infrastructure. *Climatic Change, 116*(2), 411–423.

Graf, W. L. (1999). Dam nation: A geographic census of American dams and their large-scale hydrologic impacts. *Water Resources Research, 35*(4), 1305–1311.

Graf, W. L. (2006). Downstream hydrologic and geomorphic effects of large dams on American rivers. *Geomorphology, 79*(3–4), 336–360.

Hens, L., Thinh, N. A., Hanh, T. H., Cuong, N. S., Lan, T. D., Van Thanh, N., & Le, D. T. (2018). Sea-level rise and resilience in Vietnam and the Asia-Pacific: A synthesis. *Vietnam Journal of Earth Sciences, 40*(2), 126–152.

Hirabayashi, Y., Mahendran, R., Koirala, S., Konoshima, L., Yamazaki, D., Watanabe, S., Kim, H., & Kanae, S. (2013). Global flood risk under climate change. *Nature Climate Change, 3*(9), 816–821.

ICOLD. (1998). *World register of dams*.

Islam, A. R. M., Talukdar, S., Mahato, S., Ziaul, S., Eibek, K. U., Akhter, S., Pham, Q. B., Mohammadi, B., Karimi, F., & Linh, N. T. T. (2021). Machine learning algorithm-based risk assessment of riparian wetlands in Padma River Basin of Northwest Bangladesh. *Environmental Science and Pollution Research, 28*(26), 34450–34471.

Khosravi, K., Shahabi, H., Pham, B. T., Adamowski, J., Shirzadi, A., Pradhan, B., Dou, J., Ly, H. B., Gróf, G., Ho, H. L., & Hong, H. (2019). A comparative assessment of flood susceptibility modeling using multi-criteria decision-making analysis and machine learning methods. *Journal of Hydrology, 573*, 311–323.

Kondolf, G. M. (1994). Geomorphic and environmental effects of instream gravel mining. *Landscape and Urban Planning, 28*(2–3), 225–243.

Lee, E. H., & Kim, J. H. (2018). Development of a flood-damage-based flood forecasting technique. *Journal of Hydrology, 563*, 181–194.

Leopold, L. B. (1956). Land use and sediment. *Man's Role in Changing the Face of the Earth, 2*, 639–647.

McFeeters, S. K. (1996). The use of the Normalized Difference Water Index (NDWI) in the delineation of open water features. *International Journal of Remote Sensing, 17*(7), 1425–1432.

Moraes, R., & Molander, S. (2004). A procedure for ecological tiered assessment of risks (PETAR). *Human and Ecological Risk Assessment, 10*(2), 349–371.

Naikoo, M. W., Talukdar, S., Ishtiaq, M., & Rahman, A. (2023). Modelling built-up land expansion probability using the integrated fuzzy logic and coupling coordination degree model. *Journal of Environmental Management, 325*, 116441.

Nilsson, C., Reidy, C. A., Dynesius, M., & Revenga, C. (2005). Fragmentation and flow regulation of the world's large river systems. *Science, 308*(5720), 405–408.

O'Brien, G. C., & Wepener, V. (2012). Regional-scale risk assessment methodology using the Relative Risk Model (RRM) for surface freshwater aquatic ecosystems in South Africa. *Water SA, 38*(2), 153–166.

Organization for Economic Cooperation & Development, and OECD Group of the Council on Rural Development. (1993). *What future for our countryside?: A rural development policy*. Organisation for Economic Co-operation and Development.

Pal, S., & Talukdar, S. (2018). Drivers of vulnerability to wetlands in Punarbhaba river basin of India-Bangladesh. *Ecological Indicators, 93*, 612–626.

Pal, S., & Talukdar, S. (2019). Impact of missing flow on active inundation areas and transformation of parafluvial wetlands in Punarbhaba–Tangon river basin of Indo-Bangladesh. *Geocarto International, 34*(10), 1055–1074.

Paul, G. C., Saha, S., & Hembram, T. K. (2019). Application of the GIS-based probabilistic models for mapping the flood susceptibility in Bansloi sub-basin of Ganga-Bhagirathi river and their comparison. *Remote Sensing in Earth Systems Sciences, 2*(2), 120–146.

Paul, S., & Pal, S. (2020). Exploring wetland transformations in moribund deltaic parts of India. *Geocarto International, 35*(16), 1873–1894.

Pal, S., & Saha, T. K. (2018). Identifying dam-induced wetland changes using an inundation frequency approach: The case of the Atreyee River basin of Indo-Bangladesh. *Ecohydrology & Hydrobiology, 18*(1), 66–81.

Quirogaa, V. M., Kurea, S., Udoa, K., & Manoa, A. (2016). Application of 2D numerical simulation for the analysis of the February 2014 Bolivian Amazonia flood: Application of the new HEC-RAS version 5. *Ribagua, 3*(1), 25–33.

Rashid, B., Islam, S. U., & Islam, B. (2015). Evidences of Neotectonic activities as reflected by drainage characteristics of the Mahananda River floodplain and its adjoining areas, Bangladesh. *American Journal of Earth Sciences, 2*(4), 61–70.

Rasyid, A. R., Bhandary, N. P., & Yatabe, R. (2016). Performance of frequency ratio and logistic regression model in creating GIS based landslides susceptibility map at Lompobattang Mountain, Indonesia. *Geoenvironmental Disasters, 3*(1), 19.

Samanta, S., Pal, D. K., & Palsamanta, B. (2018). Flood susceptibility analysis through remote sensing, GIS and frequency ratio model. *Applied Water Science, 8*(2), 1–14.

Sarkar, D., & Mondal, P. (2020). Flood vulnerability mapping using frequency ratio (FR) model: A case study on Kulik river basin, indo-Bangladesh Barind region. *Applied Water Science, 10*(1), 1–13.

Sevgen, E., Kocaman, S., Nefeslioglu, H. A., & Gokceoglu, C. (2019). A novel performance assessment approach using photogrammetric techniques for landslide susceptibility mapping with logistic regression, ANN and random forest. *Sensors, 19*(18), 3940.

Solaimani, K., Mousavi, S. Z., & Kavian, A. (2013). Landslide susceptibility mapping based on frequency ratio and logistic regression models. *Arabian Journal of Geosciences, 6*(7), 2557–2569.

Süzen, M. L., & Doyuran, V. (2004). A comparison of the GIS based landslide susceptibility assessment methods: Multivariate versus bivariate. *Environmental Geology, 45*(5), 665–679.

Talukdar, S., & Pal, S. (2017). Impact of dam on inundation regime of flood plain wetland of punarbhaba river basin of barind tract of Indo-Bangladesh. *International Soil and Water Conservation Research, 5*(2), 109–121.

Talukdar, S., & Pal, S. (2018). Impact of dam on flow regime and flood plain modification in Punarbhaba River Basin of Indo-Bangladesh Barind tract. *Water Conservation Science and Engineering, 3*(2), 59–77.

Talukdar, S., Pal, S., Chakraborty, A., & Mahato, S. (2020). Damming effects on trophic and habitat state of riparian wetlands and their spatial relationship. *Ecological Indicators, 118*, 106757.

Talukdar, S., & Pal, S. (2021). *Impact of hydrological alteration of riparian wetlands in Punarbhaba river basin of Indo-Bangladesh (unpublished thesis).* University of Gour Banga.

Talukdar, S., Pal, S., Shahfahad., Naikoo, M.W., Parvez, A., Rahman, A. (2023). Trend analysis and forecasting of streamflow using random forest in the Punarbhaba River basin. Environmental Monitoring and Assessment, 195(1), 153.

Tehrany, M. S., Pradhan, B., & Jebuv, M. N. (2014). A comparative assessment between object and pixel-based classification approaches for land use/land cover mapping using SPOT 5 imagery. *Geocarto International, 29*(4), 351–369.

Tonina, D., & Jorde, K. (2013). *Hydraulic modeling approaches for ecohydraulic studies: 3D, 2D, 1D and non-numerical models* (pp. 31–66). An integrated approach.

Townshend, J. R., & Justice, C. O. (1986). Analysis of the dynamics of African vegetation using the normalized difference vegetation index. *International Journal of Remote Sensing, 7*(11), 1435–1445.

USACE. (1993). *Engineering Manual EM 1110–2-1415, Chapter 3*. Flood Frequency Analysis, US Army Corps of Engineers.

USEPA (US Environmental Protection Agency). (1998). *Method 3051a—Microwave assisted acid digestion of sediments, sludges, soils, and oils*.

Walker, R., Landis, W., & Brown, P. (2001). Developing a regional ecological risk assessment: A case study of a Tasmanian agricultural catchment. *Human and Ecological Risk Assessment, 7*(2), 417–439.

Williams, G. P., & Wolman, M. G. (1984). *Downstream effects of dams on alluvial rivers* (Vol. 1286). US Government Printing Office.

World Commission on Dams. (2000). Dams and development: A new framework for decision-making. In *A report of the World Commission on Dams*. Earthscan. http:/www.dams.org/report. Accessed 5 Sept 2004.

Wu, Z., Zhou, Y., Wang, H., & Jiang, Z. (2020). Depth prediction of urban flood under different rainfall return periods based on deep learning and data warehouse. *Science of the Total Environment, 716*, 137077.

Xu, H. (2006). Modification of normalised difference water index (NDWI) to enhance open water features in remotely sensed imagery. *International Journal of Remote Sensing, 27*(14), 3025–3033.

Yalcin, G., & Akyurek, Z. (2004, July). Analysing flood vulnerable areas with multicriteria evaluation. In *20th ISPRS Congress* (pp. 359–364).